Electronic Supplementary Information

Chromium ion pair luminescence with controllable coupling strength

Xuewan Lin[a], Long Chen[a] and Jiyou Zhong[a,b]*

[a]School of Physics and Optoelectronic Engineering, Guangdong University of Technology, Guangzhou 510006, China. E-mail: jyzhong2016@gdut.edu.cn.

[b]Guangdong Provincial Key Laboratory of Sensing Physics and System Integration Applications, Guangdong University of Technology, Guangzhou 510006, China.

Experimental Section

***Synthesis*:** The polycrystalline powder of $K_2Zr_{1-\delta}Ti_\delta Al_{1-x}(PO_4)_3:xCr^{3+}$ (δ= 0, 0.2, 0.4, 0.6, 0.8, and 1; *x*=0 and 0.06) were synthesized by conventional high-temperature solid-state reaction method. The K_2CO_3 (Aladdin, 99.95%), ZrO_2 (Aladdin, 99.99%), TiO_2 (Aladdin, 99.99%), Al_2O_3 (Aladdin, 99.99%), $NH_4H_2PO_4$ (Aladdin, 99.99%) and Cr_2O_3 (Aladdin, 99.99%) were taken as raw materials, and were weighed according to the standard stoichiometric ratio. The weighed raw materials were ground in an agate mortar for half an hour, then the mixtures were loaded into corundum crucibles and heated at 1123 K for 6 hours in a tube furnace. The products were taken out from the cooled furnace and ground into fine powders for subsequent tests.

Characterization: The phase purity of samples were checked by X-ray diffraction (XRD) patterns collected in a diffractometer (D8 ADVANCE, Bruker). The crystal structure was determined via XRD refinement by performing GSAS software and visualized using VESTA package.[1] The electron paramagnetic resonance (EPR) spectra were collected in an EPR spectrometer (JES-FA300, Japan). The excitation, emission spectra and decay curves were collected by using a fluorescence spectrometer (FLS-1000, Edinburgh Instruments). The diffuse reflectance (DR) data was collected via an UV–vis–NIR spectrophotometer (Shimadzu, Japan). The photoluminescence quantum yield (PLQY) and absorption efficiency (AE) were measured by using an absolute photoluminescence quantum yield measurement system (Quantaurus-QY Plus C13534-11, Hamamatsu Photonics). The output parameters of the fabricated NIR pc-LED device was measured using an optoelectronic testing system (HAAS-2000, EVERFINE).

Computation: The structural models of $K_2AlX(PO_4)_3:Cr^{3+}$ (X = Zr, and Ti) were constructed with four types of neutral defect. The structure optimization, and formation energy calculations were performed via adopting DFT-PBE exchange-correlation functional performed on the Vienna ab initio Simulation Package (VASP). The basic parameters setting involving cut off energy for basis set of the plane waves, criteria for electronic and atomic convergence, and sampling the first Brillouin zone can be referenced to our previous work.[2]

Supplementary Equations

The crystal field strength parameter (*Dq*/*B*) estimated by the following equations: [3]

$$10\mathrm{Dq} = \mathrm{E}(^4\mathrm{A}_2 \rightarrow {}^4\mathrm{T}_2) \quad \textbf{(Eqn. S1)}$$

$$Dq/B = \frac{15(m-8)}{m^2 - 10m} \quad \textbf{(Eqn. S2)}$$

$$m = \frac{E(^4A_2 \rightarrow {}^4T_1) - E(^4A_2 \rightarrow {}^4T_2)}{Dq} \quad \textbf{(Eqn. S3)}$$

where *Dq* and *B* represents crystal field splitting energy and the Racah parameter, respectively; while $E(^4A_2 \rightarrow {}^4T_1)$ and $E(^4A_2 \rightarrow {}^4T_2)$ correspond to the peak positions of the excitation bands of the $^4T_1$ and $^4T_2$ levels.

The Huang-Rhys factor (S) is obtained by fitting the following equation:[4]

$$\mathrm{fwhm\ (T)} = \sqrt{8\ln 2} \times \mathrm{hv} \times \sqrt{\coth\ (\mathrm{hv}/2\mathrm{kT})} \quad \textbf{(Eqn. S4)}$$

where the hv and k are the phonon energy and Boltzmann's constant, respectively.

Supplementary Figures and Tables

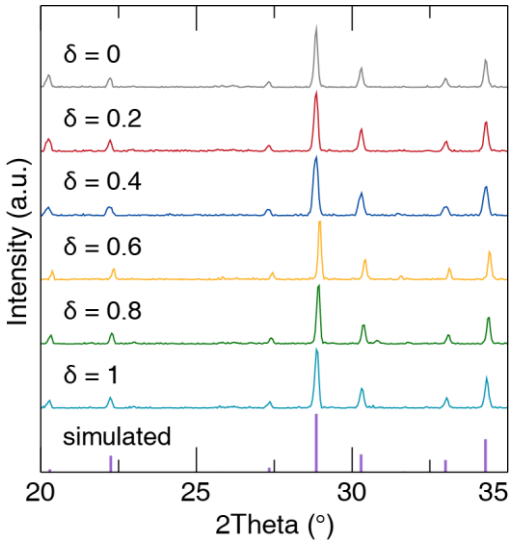

Fig. S1. XRD patterns of the $K_2Zr_{1-\delta}Ti_\delta Al_{0.94}(PO_4)_3$:0.06$Cr^{3+}$ (δ= 0, 0.2, 0.4, 0.6, 0.8, and 1) solid-solutions compared with the standard XRD pattern.

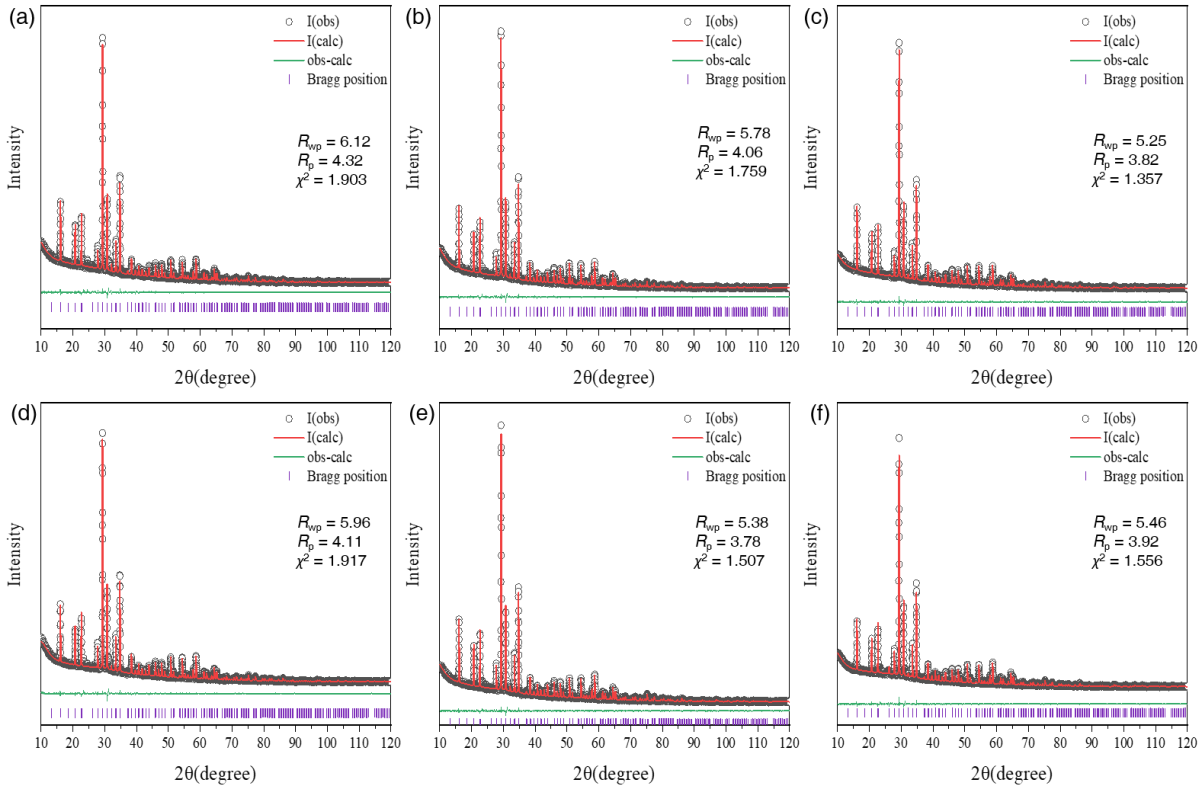

Fig. S2. (a-f) Rietveld refinement of XRD pattern for $K_2Zr_{1-\delta}Ti_\delta Al_{0.94}(PO_4)_3$:0.06$Cr^{3+}$ (δ= 0, 0.2, 0.4, 0.6, 0.8, and 1) samples.

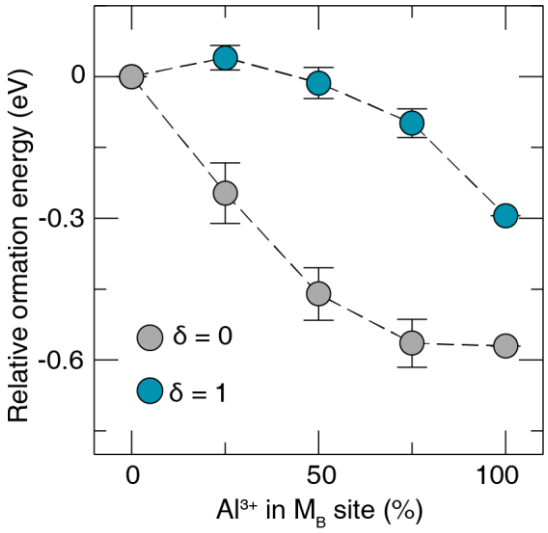

Fig. S3. Relative formation energy for $K_2XAl(PO_4)_3$ (X = Zr, Ti) calculated by DFT functional.

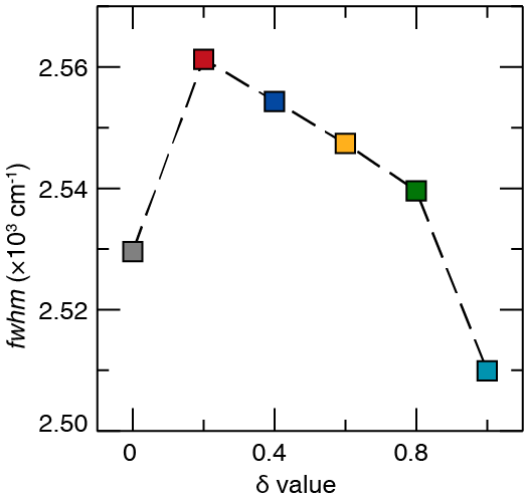

Fig. S4. The fwhm of $K_2Zr_{1-\delta}Ti_{\delta}Al_{0.94}(PO_4)_3$:0.06$Cr^{3+}$ (δ= 0, 0.2, 0.4, 0.6, 0.8, and 1) samples.

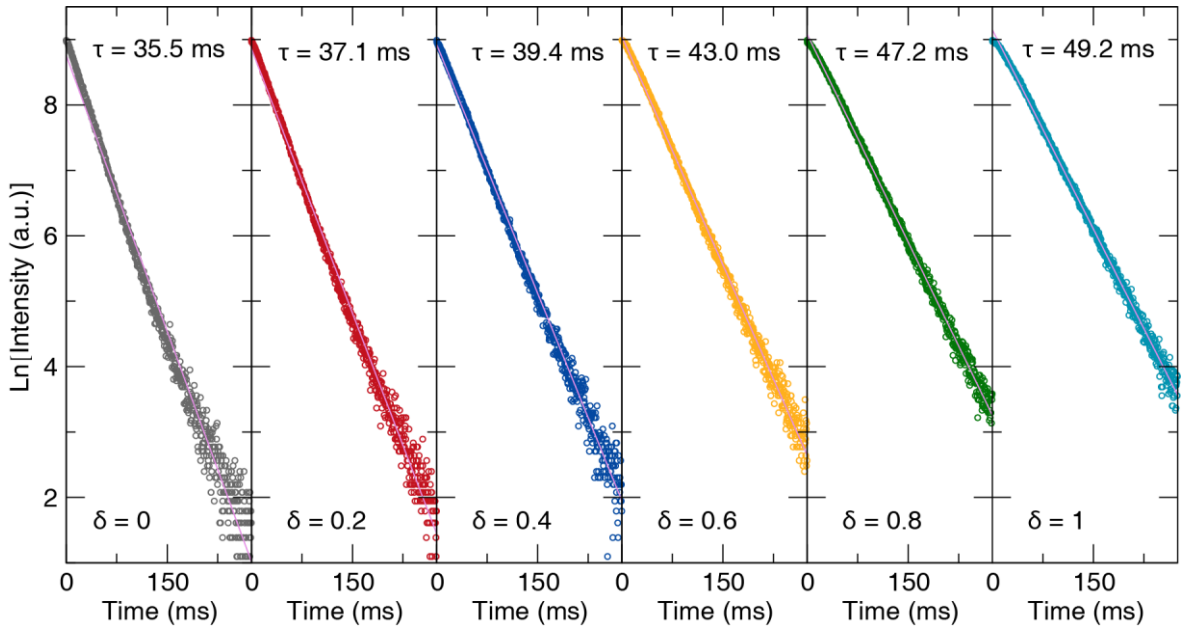

Fig. S5. Decay curves of $K_2Zr_{1-\delta}Ti_{\delta}Al_{0.94}(PO_4)_3$:0.06$Cr^{3+}$ (δ= 0, 0.2, 0.4, 0.6, 0.8, and 1) fitted by a single exponential function.

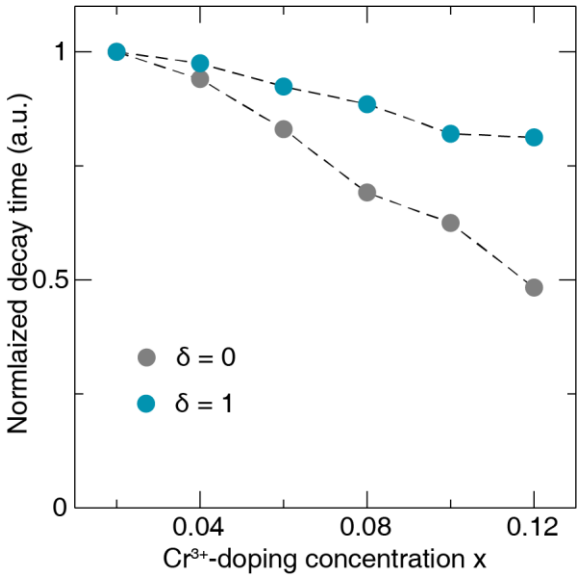

Fig. S6. Normalized decay time at different Cr^{3+} doping concentration of $K_2Zr_{1-\delta}Ti_\delta Al_{1-x}(PO_4)_3$:$xCr^{3+}$ with (a) δ= 0, and (b) δ= 1.

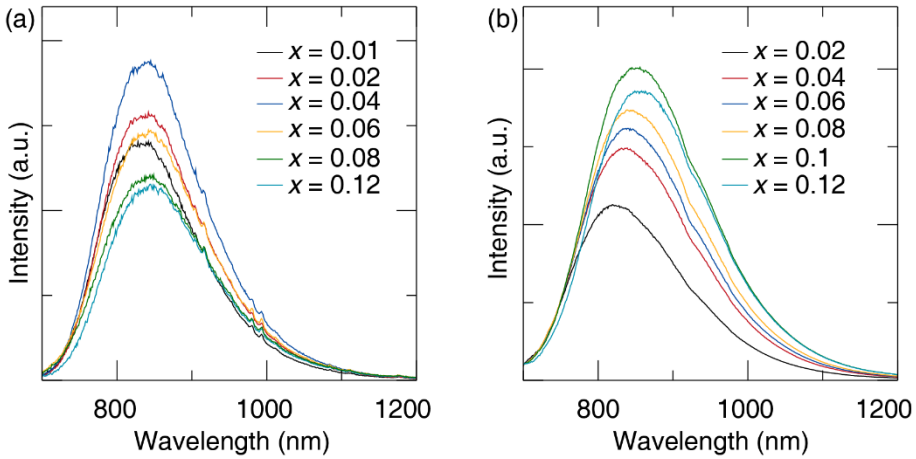

Fig. S7. Emission spectra at different Cr^{3+} doping concentration of $K_2Zr_{1-\delta}Ti_\delta Al_{1-x}(PO_4)_3$:$xCr^{3+}$ with (a) δ= 0, and (b) δ= 1.

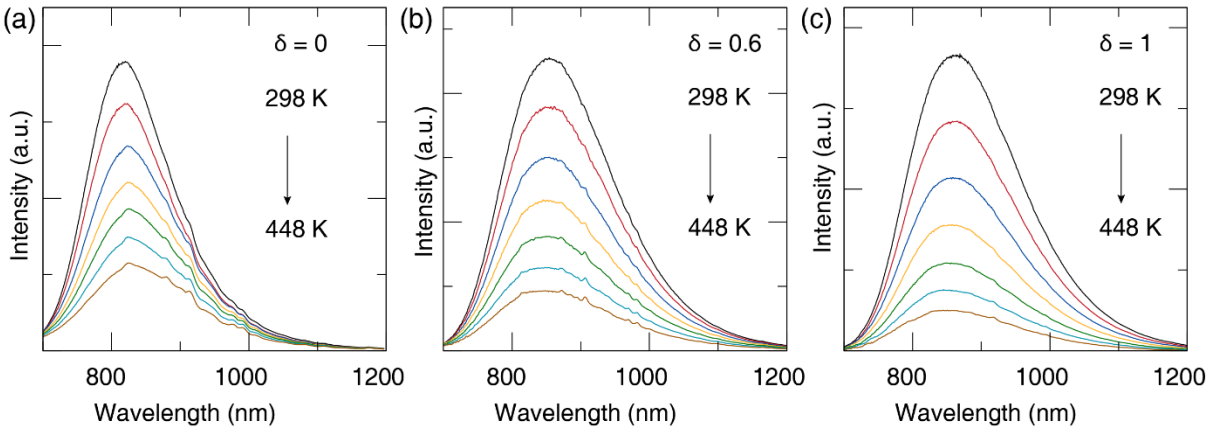

Fig. S8. (a-c) Temperature-dependent emission spectra of $K_2Zr_{1-\delta}Ti_{\delta}Al_{0.94}(PO_4)_3$:0.06$Cr^{3+}$ (δ= 0, 0.6, and 1) samples.

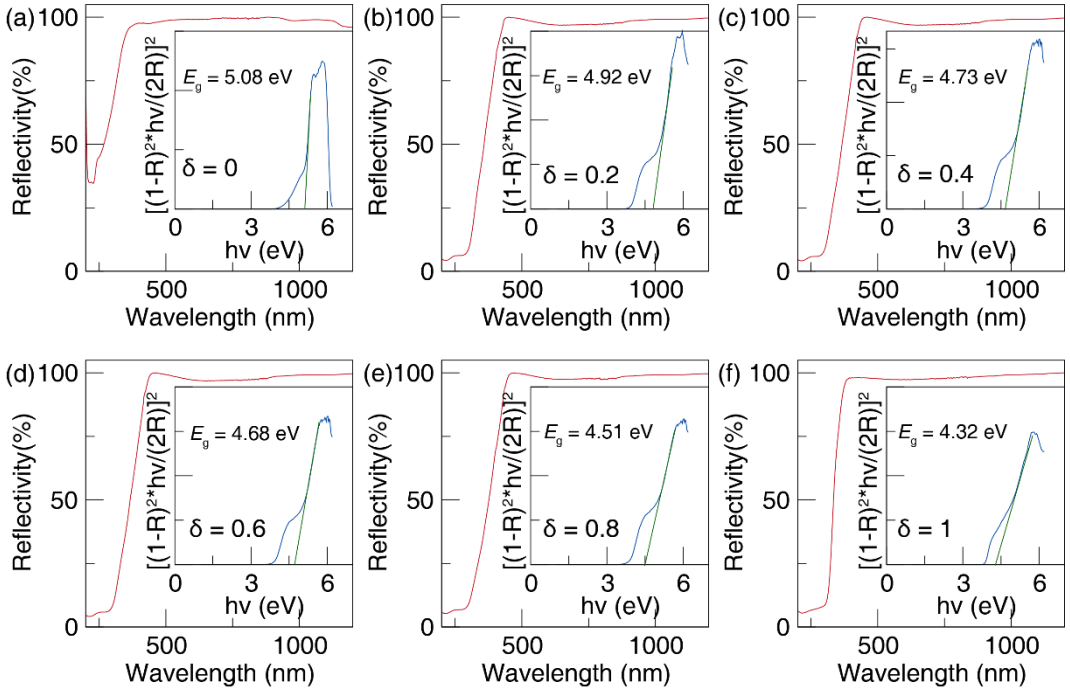

Fig. S9. (a-f) DR spectra and calculated optical band gap of $K_2Zr_{1-\delta}Ti_{\delta}Al(PO_4)_3$ (δ= 0, 0.2, 0.4, 0.6, 0.8, and 1) hosts.

Table S1 Refined Results of $K_2Zr_{1-\delta}Ti_{\delta}Al_{0.94}(PO_4)_3$:0.06$Cr^{3+}$ (δ= 0, 0.2, 0.4, 0.6, 0.8, and 1) Samples.

δ value	δ = 0	δ = 0.2	δ = 0.4	δ = 0.6	δ = 0.8	δ = 1
Radiation type; λ (Å)	X-ray; 1.5406	X-ray; 1.5406	X-ray; 1.5406	X-ray; 1.5406	X-ray; 1.5406	X-ray; 1.5406
2θ (degree)	10 - 120	10 - 120	10 - 120	10 - 120	10 - 120	10 - 120
Temperature (K)	298	298	298	298	298	298
Space group	$P2_13$	$P2_13$	$P2_13$	$P2_13$	$P2_13$	$P2_13$
$\alpha = \beta = \gamma$ (degree)	90.00	90.00	90.00	90.00	90.00	90.00
$a = b = c$ (Å)	9.83820(9)	9.82246(6)	9.79647(5)	9.77949(3)	9.75705(6)	9.73148(8)
V (Å^3)	952.24(4)	947.68(6)	940.17(7)	935.29(6)	928.87(3)	921.5(9)
Profile R-factor, R_p (%)	0.0432	0.0406	0.382	0.0411	0.0378	0.0392
Weighted profile R-factor, R_{wp} (%)	0.0612	0.0578	0.0525	0.0596	0.0538	0.0546
χ^2	1.903	1.759	1.357	1.917	1.507	1.556

Supplementary References

1 B. H. Toby, *J. Appl. Crystallogr.*, 2001, **34**, 210–213.
2 L. Chen and J. Zhong, *ACS Appl. Mater. Interfaces*, 2024, **16**, 41119–41126.
3 B. Struve and G. Huber, *Appl. Phys. B Photophysics Laser Chem.*, 1985, **36**, 195–201.
4 C. Liu, Z. Qi, C.-G. Ma, P. Dorenbos, D. Hou, S. Zhang, X. Kuang, J. Zhang and H. Liang, *Chem. Mater.*, 2014, **26**, 3709–3715.